

A Study of Final State Interaction in the ${}^3\text{He}(e, e'p){}^2\text{H}(np)$ and ${}^4\text{He}(e, e'p){}^3\text{H}$ Reaction

C. Ciofi degli Atti¹, L. P. Kaptari², and H. Morita³

¹ Department of Physics, University of Perugia and Istituto Nazionale di Fisica Nucleare, Sezione di Perugia, Via A. Pascoli, I-06123, Italy

² Bogoliubov Lab. Theor. Phys., 141980, JINR, Dubna, Russia

³ Sapporo Gakuin University, 11 Bunkyo-dai, Ebetsu-shi, Hokkaido 069-8555, Japan

Abstract. We have investigated the propagation of the knocked out proton in the exclusive process $A(e, e'p)B$ in few-nucleon systems using realistic nuclear wave functions and Glauber multiple scattering theory both in its original form and within a generalized eikonal approximation. New results for the processes ${}^3\text{He}(e, e'p){}^2\text{H}(pn)$ and ${}^4\text{He}(e, e'p){}^3\text{H}$ are compared with data recently obtained at the Thomas Jefferson Laboratory (JLAB). The results suggest that the Glauber approach describes well the proton propagation, in other words the final state interaction(FSI) in the considered experimental region. Possible occurrence of the color transparency effect is also discussed within the concept of the finite formation time(FFT) effect.

1 Introduction

Exclusive and semi-inclusive lepton scattering off nuclei $A(l, l'p)X$ in the quasi elastic region, play a relevant role in nowadays hadronic physics, mainly for three reasons: i) by virtue of the wide kinematical range available by present experimental facilities detailed information on nuclei (e.g. nucleon-nucleon (NN) correlations) can be obtained; ii) the mechanism of propagation of hadronic states can be investigated in great details; iii) at high energies color transparency effects, which has attracted many researcher's interest, might be investigated. The key point in the treatment of $A(l, l'p)X$ process is the determination of the propagation of the produced hadrons in the medium, which is usually referred to as the problem of the Final State Interaction (FSI). On the other hand, at medium and high energies hadron propagation is usually treated within the Glauber multiple scattering approach (GA), which has been applied with great success to hadron scattering off nuclear targets [1]. Therefore the GA has been naturally applied also for the process $A(l, l'p)X$, where the hadron is created inside the nucleus, advocating improvements of the original GA. Most of them are based upon a Feynman diagram reformulation of the GA; such a diagrammatic approach, has been developed long ago for the case of hadron-nucleus scattering [2] and it has been generalized to the process $A(l, l'p)X$ [3, 4], showing that in particular kinematical regions it predicts appreciable deviations from original GA. In such an approach based upon a generalized eikonal approximation (GEA), the *frozen approximation*, common to GA, is partly removed by taking into account the excitation energy of the $(A - 1)$

system, which results in a correction term to the standard profile function of GA. The GEA has recently been applied to a systematic calculation of the exclusive processes ${}^3\text{He}(e, e'p){}^2\text{H}$ and ${}^3\text{He}(e, e'p)(np)$ [5, 6] using realistic three-body wave functions [7] and two-nucleon interactions (AV18) [8]; the results of calculations show a nice agreement with recent Thomas Jefferson Laboratory (JLAB) data [9]. The two-body break up channel ${}^3\text{He}(e, e'p){}^2\text{H}$ has also been considered within the Glauber approach in [10], obtaining results consistent with [5, 6]. The aim of this contribution is twofold: i) to extend the GEA calculation to the four-body system, namely to the calculation of the process ${}^4\text{He}(e, e'p){}^3\text{H}$, for which data have been obtained recently at JLAB [11]; ii) to consider for the same reaction, through the concept of Finite Formation Time (FFT) as developed in [13], the role played by nucleon virtuality which is expected to become important at high values of Q^2 . Our paper is organized as follows: in Section 2 the basic elements of our theoretical framework are given; the comparison of our results with experimental data on ${}^3\text{He}(e, e'p){}^2\text{H}(pn)$ and ${}^4\text{He}(e, e'p){}^3\text{H}$ reactions are presented in Section 3; FFT effects on the process ${}^4\text{He}(e, e'p){}^3\text{H}$ are illustrated in Section 4; the Summary and Conclusions are given in Section 5.

2 The Cross Section for the Process $A(e, e'p)B$ within GA and GEA

The FSI which is considered in the diagrammatic approach of [3–6] is the elastic scattering of the hit nucleon by the nucleons of the spectator $A - 1$. Under two main assumptions which are expected to be valid at medium and high energies, namely that: i) in each rescattering process the momentum transfer is small, and ii) the spin flip part of the NN scattering amplitude can be disregarded, the method predicts that nuclear effects in the exclusive process $A(e, e'p)B$ should be governed by the Distorted Spectral Function

$$P_A^{\text{FSI}}(\mathbf{p}_m, E_m) = \frac{1}{(2\pi)^3} \frac{1}{2J_A + 1} \sum_f \sum_{\mathcal{M}_A, \mathcal{M}_{A-1}, s_1} \times \\ \times \left| \sum_{n=0}^{A-1} \mathcal{T}_A^{(n)}(\mathcal{M}_A, \mathcal{M}_{A-1}, s_1; f) \right|^2 \delta(E_m - (E_{A-1}^f + E_{\text{min}})) \quad (1)$$

where $\mathbf{p}_m = \mathbf{P}_{A-1} = \mathbf{q} - \mathbf{p}_1$ and E_m are the *missing momentum* and *missing energy*, respectively (here \mathbf{p}_1 and \mathbf{q} are the momentum of the detected nucleon and the 3-momentum transfer, respectively, and $E_{\text{min}} = E_A - E_{A-1}$, E_A and E_{A-1} being the positive ground state energies of A and $(A - 1)$ system); \mathcal{M}_A , \mathcal{M}_{A-1} , and s_1 , are magnetic quantum numbers; the sum over f stands for a sum over all possible discrete and continuum states of the $(A - 1)$ system; $\mathcal{T}_A^{(n)}$ represents the reduced (Lorentz index independent) amplitude which, at order n , takes into account all possible diagrams describing n -body rescattering (see [5]). In the case of

${}^3\text{He}$, after the evaluation of all single and double scattering diagrams, the distorted spectral function reads as follows

$$\begin{aligned}
P_3^{\text{FSI}}(\mathbf{p}_m, E_m) &= \frac{1}{2(2\pi)^3} \sum_{f=D, np} \sum_{\mathcal{M}_3, \mathcal{M}_2, s_1} \times \\
&\times \left| \int e^{i\boldsymbol{\rho} \cdot \mathbf{p}_m} \chi_{\frac{1}{2}s_1}^\dagger \Psi_f^{\mathcal{M}_2 \dagger}(\mathbf{r}) \mathcal{S}_{\text{GEA}}(\boldsymbol{\rho}, \mathbf{r}) \Psi_{\text{He}}^{\mathcal{M}_3}(\boldsymbol{\rho}, \mathbf{r}) d\boldsymbol{\rho} d\mathbf{r} \right|^2 \times \\
&\times \delta(E_m - (E_{A-1}^f + E_{\text{min}}))
\end{aligned} \quad (2)$$

where $E_{A-1}^f + E_{\text{min}} = E_{\text{min}}$ for the two-body break up (2buu) channel ($f = D$), and $E_{A-1}^f + E_{\text{min}} = \mathbf{t}^2/M_N + E_3$ for the three-body break up (3buu) ($f = (np)$) channel (here \mathbf{t} is the relative momentum of the interacting ($n-p$) pair in the continuum). The quantity \mathcal{S}_{GEA} introduces FSI and has the form $\mathcal{S}_{\text{GEA}} = \mathcal{S}_{\text{GEA}}^{(1)} + \mathcal{S}_{\text{GEA}}^{(2)}$, with

$$\mathcal{S}_{\text{GEA}}^{(1)}(\boldsymbol{\rho}, \mathbf{r}) = 1 - \sum_{i=2}^3 \theta(z_i - z_1) e^{i\Delta_z(z_i - z_1)} \Gamma(\mathbf{b}_1 - \mathbf{b}_i) \quad (3)$$

and

$$\begin{aligned}
\mathcal{S}_{\text{GEA}}^{(2)}(\boldsymbol{\rho}, \mathbf{r}) &= \left[\theta(z_2 - z_1) \theta(z_3 - z_2) e^{-i\Delta_3(z_2 - z_1)} e^{-i(\Delta_3 + \Delta_z)(z_3 + z_1)} + \right. \\
&\quad \left. + \theta(z_3 - z_1) \theta(z_2 - z_3) e^{-i\Delta_2(z_3 - z_1)} e^{-i(\Delta_2 + \Delta_z)(z_2 - z_1)} \right] \times \\
&\quad \times \Gamma(\mathbf{b}_1 - \mathbf{b}_2) \Gamma(\mathbf{b}_1 - \mathbf{b}_3)
\end{aligned} \quad (4)$$

where $\Delta_i = (q_0/|\mathbf{q}|)(E_{\mathbf{k}_i} - E_{\mathbf{k}'_i})$ and $\Delta_z = (q_0/|\mathbf{q}|)E_m$, $\mathbf{k}_i, \mathbf{k}'_i$, being nucleon momenta before and after the rescattering. The profile function $\Gamma(\mathbf{b})$ is given by

$$\Gamma(\mathbf{b}) = \frac{\sigma_{NN}^{\text{tot}}(1 - i\alpha_{NN})}{4\pi b_0^2} e^{-\mathbf{b}^2/2b_0^2}, \quad (5)$$

which is the standard parametrization. It can be seen that Δ_z takes into account Fermi motion and therefore partly remove the frozen approximation. Note that when $\Delta_i = \Delta_z = 0$, the usual GA is recovered.

Finally the expression of the differential cross section, which assumes a factorized form, can be given by

$$\frac{d^6\sigma}{d\nu d\Omega_e dp d\Omega_p} = \mathcal{K} \sigma_{ep} P_A^{\text{FSI}}(\mathbf{p}_m, E_m), \quad (6)$$

where \mathcal{K} is a kinematical factor, σ_{ep} the electron-nucleon cross section and ν the energy transfer.

3 Calculations of the Processes ${}^3\text{He}(e, e'p){}^2\text{H}(pn)$ and ${}^4\text{He}(e, e'p){}^3\text{H}$ Reaction

According to the formulation given above we have calculated the cross sections of the processes ${}^3\text{He}(e, e'p){}^2\text{H}$, ${}^3\text{He}(e, e'p)(np)$. All the parameters in the profile function, appeared in Eq. (5), are taken from [12]. For the electron-nucleon cross section σ_{ep} we used the De Forest $\sigma_{ep}^{cc1}(\bar{Q}^2, \mathbf{p}_m)$ cross section [15]. All two-, three-, and four-body wave functions are direct solutions of the non relativistic Schrödinger equation, therefore our calculations are fully parameter free.

In the case of the three-nucleon system, the results for the 2bbu and 3bbu channels are shown in Figures 1 and 2 [6]. Figure 1 shows that the missing momentum dependence of the experimental cross section clearly exhibits different slopes, that are reminiscent of the slopes observed in elastic hadron-nucleus scattering at intermediate energies (see e.g. [1]) and our parameter free calculations demonstrate that: i) these slopes are indeed related to multiple scattering in the final state, and ii) a highly satisfactory agreement between theory and experiment is obtained including the 3bbu case, which means that in the energy-momentum range covered by the data, FSI can be described by elastic rescattering; iii) GA and GEA, differ only by a few percent therefore we do not show the curve for the GEA separately.

In the case of ${}^4\text{He}$, which has $\mathcal{S}_{\text{GEA}} = \mathcal{S}_{\text{GEA}}^{(1)} + \mathcal{S}_{\text{GEA}}^{(2)} + \mathcal{S}_{\text{GEA}}^{(3)}$, we have used realistic variational wave functions for both ${}^4\text{He}$ and ${}^3\text{H}$ [16, 17], corresponding to the RSC V8 model potential [18]. The results for the reduced cross section

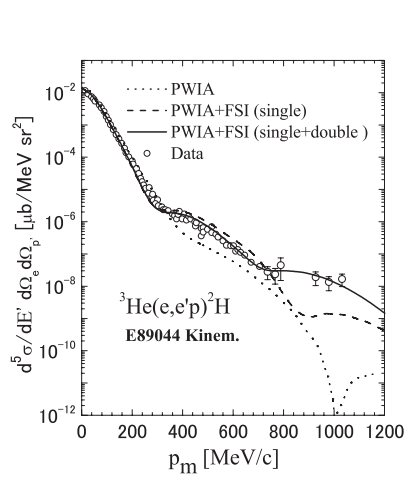


Figure 1. Results for the ${}^3\text{He}(e, e'p){}^2\text{H}$ reaction [6]. Dotted curve: PWIA result; dashed curve: FSI (single rescattering); solid curve: FSI (single plus double rescattering). Experimental data from [9].

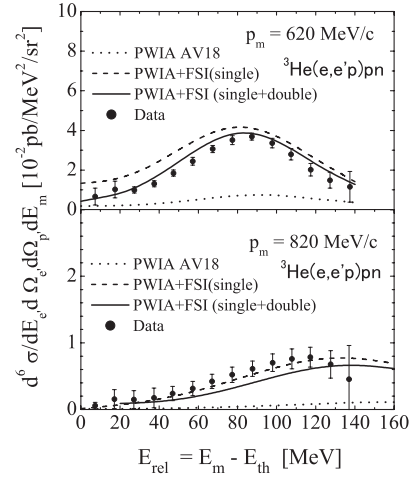


Figure 2. The same as in Figure 1 but for the process ${}^3\text{He}(e, e'p)pn$ ($E_{\text{th}} = E_3$ is the two-nucleon emission threshold in ${}^3\text{He}$).

$$n_D(\mathbf{p}_m) = \frac{d^5\sigma}{d\omega d\Omega_e d\Omega_p} (\mathcal{K}\sigma_{ep})^{-1}, \quad (7)$$

are compared with the JLab E97111 experimental data in parallel(Py2) and perpendicular (CQ ω 2) kinematics [11], in Figures 3 and 4 respectively. Figure 3 shows that: i) the dip predicted by the PWIA is totally filled up by the FSI; ii) like the ${}^3\text{He}$ case, the difference between GA and GEA is very small; iii) although we predict an overall satisfactory behavior of the experimental data in parallel kinematics, we systematically underestimate them, on its reason we are still studying. In case of perpendicular kinematics, shown in Figure 4, the agreement between theory and experiment is much better and the differences between GA and GEA are more pronounced, though still it is much smaller than the error bar.

The multiple scattering contributions are illustrated in Figure 5. As the case of ${}^3\text{He}$ the single rescattering amplitude dominates at $p_m \leq 600$ MeV/c whereas at higher values of p_m multiple scattering effects become important, with the triple rescattering term contributing significantly at $p_m > 800$ MeV/c. Before closing this section, let us mention about the choice of the z -axis. In our calculations we have always directed the z -axis along the momentum of the propagating nucleon \mathbf{p}_1 . In several Glauber-type calculations the z -axis is chosen along \mathbf{q} , assuming $|\mathbf{q}|$ to be large enough. However Figure 6 shows that this is not the case in the JLAB kinematics, and the calculation with the z -axis directed along \mathbf{q} underestimates the

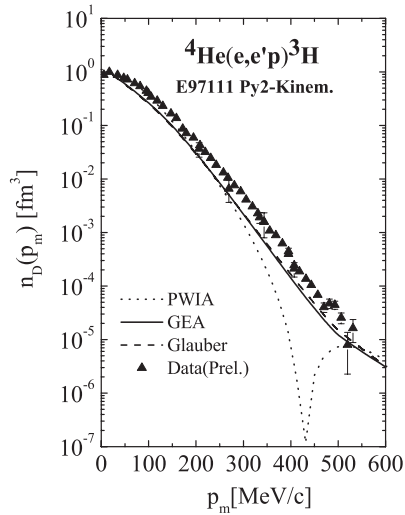


Figure 3. The reduced cross section $n_D(\mathbf{p}_m) = [d^5\sigma/(d\omega d\Omega_e d\Omega_p)] \times [\mathcal{K}\sigma_{ep}]^{-1}$ for the process ${}^4\text{He}(e, e'p){}^3\text{H}$ in parallel kinematics. Preliminary data from [11].

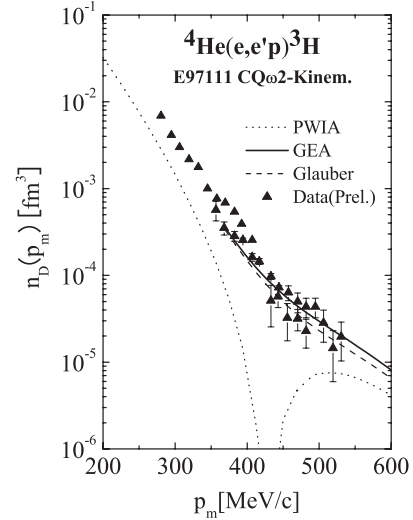


Figure 4. The same as in Figure 3 but for perpendicular kinematics.

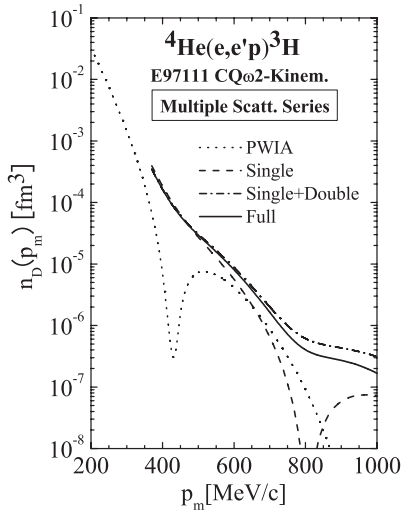


Figure 5. Multiple scattering contributions in the process ${}^4\text{He}(e, e'p){}^3\text{H}$. The results are similar to the ones shown in Figure 1, but in this case triple rescattering contributions start to contribute at $p_m \geq 800$ MeV/c.

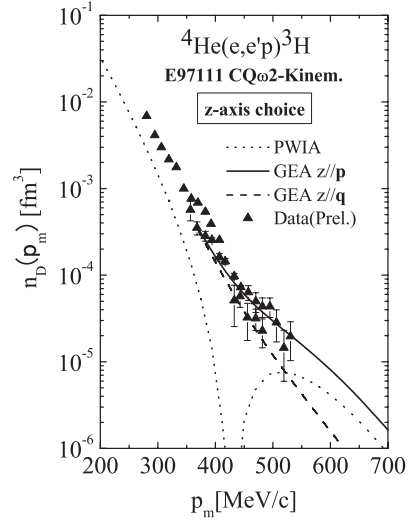


Figure 6. The choice of z -axis for the Glauber operator. The dashed curve corresponds to the calculation with the z -axis along the direction of \mathbf{q} . See text. Preliminary data from [11]

correct results by a large factor. This clearly reveals that a correct choice of the z -axis is crucially important in applying the GA to the $(e, e'p)$ process.

4 Finite Formation Time Effects in the Process ${}^4\text{He}(e, e'p){}^3\text{H}$

It has been argued by various authors that at high values of Q^2 the phenomenon of color transparency, i.e. a reduced NN cross section in the medium, might be observed. Color transparency is a consequence of the cancellation between various hadronic intermediate states of the produced ejectile. In [13] the vanishing of FSI at Q^2 has been produced by considering the finite formation time (FFT) the ejectile needs to reach its asymptotic form of a physical baryon. This has been implemented by explicitly considering the virtuality dependence of the NN scattering amplitude. According to [13] FFT effects can be introduced in Eq. (2) by replacing \mathcal{S}_{GEA} with \mathcal{S}_{FFT} , given by

$$\mathcal{S}_{\text{FFT}}(1i) = 1 - J(z_i - z_1)\Gamma(\mathbf{b}_1 - \mathbf{b}_i), \quad (8)$$

$$J(z) = \theta(z) (1 - \exp(-z/l(Q^2))), \quad l(Q^2) = \frac{Q^2}{xm_N M^2} \quad (9)$$

which is obtained from \mathcal{S}_{GEA} simply by setting $\Delta_i = \Delta_z = 0$ and replacing $\theta(z)$ by $J(z)$. Where x is the Bjorken scaling variable and the quantity $l(Q^2)$ plays the

role of the proton formation length, the length of the trajectory that the knocked out proton runs until it return to its asymptotic form. The quantity M is related to the nucleon mass m_N and to an average resonance state of mass m^* by $M^2 = m^{*2} - m_N^2$; the value $m^* = 1.8$ GeV has been used in the calculations [13]. Since this formation length grows linearly with Q^2 , at higher Q^2 the strength of the Glauber-type FSI is reduced by the damping factor $(1 - \exp[-(z_i - z_1)/l(Q^2)])$ appearing in Eq. (9), which physically describes the following situation: once the hit proton virtually reaches a resonance state, it will need a finite amount of time to return to its asymptotic form, during which FSI becomes weaker than the Glauber one; if $l(Q^2) = 0$, then \mathcal{S}_{FFT} reduces to the usual Glauber operator \mathcal{S}_G . Including the FFT effects defined above, we have calculated the cross section of the process ${}^4\text{He}(e, e'p){}^3\text{H}$ in perpendicular kinematics (see also [14]). The results are presented in Figure 7, which shows that at the JLAB kinematics ($Q^2 = 1.78$ (GeV/c) 2 , $x \sim 1.8$) FFT effects, as expected, are too small to be detected.

We have therefore extended our calculation to higher values of Q^2 reducing the value of x to $x = 1.4$, because at $x \sim 1.8$ the region with $p_m < 500$ (MeV/c) is kinematically forbidden at $Q^2 \geq 5$ (GeV/c) 2 . The results, presented in Figure 8, show that FFT effects induces a large Q^2 dependence which can not be produced by the usual Glauber operator, as instructed in Figure 9. Thus, observing the Q^2 dependence of the cross section of ${}^4\text{He}(e, e'p){}^3\text{H}$ process at $p_m \sim 430$ MeV/c region up to around $Q^2 \sim 10$ (GeV/c) 2 would be of of great interest.

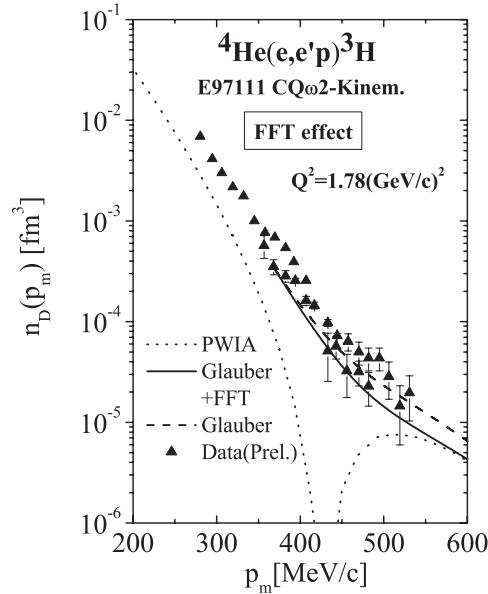


Figure 7. The FFT effect on the CQw2 kinematics. The solid line shows the results within GEA, whereas the dashed curve corresponds to the conventional GA. Preliminary data from [11].

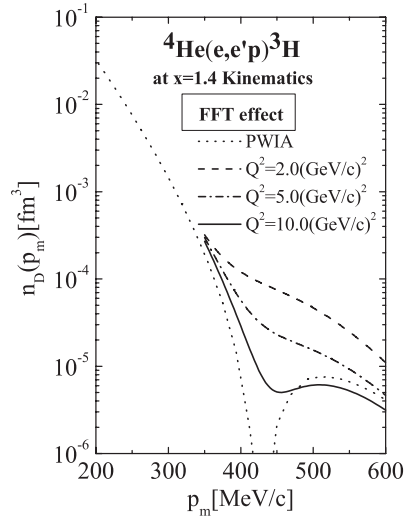


Figure 8. The Q^2 dependence of the cross section calculated by including FFT effects at $x = 1.4$ kinematics. A large Q^2 dependence appears.

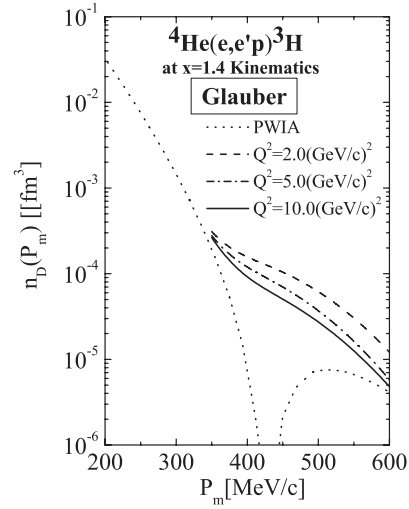


Figure 9. The same as Figure 8, but calculated with the usual Glauber operator. In this case the Q^2 dependence is much smaller than Figure 8.

5 Summary and Conclusions

We have calculated the cross section of the processes ${}^3\text{He}(e, e'p){}^2\text{H}$, ${}^3\text{He}(e, e'p)(np)$ and ${}^4\text{He}(e, e'p){}^3\text{H}$, which have been recently measured at the JLab, using realistic few-body wave functions and describing the propagation of the hit nucleon in the medium in terms of elastic rescattering. To this end we have adopted the standard Glauber approach (GA), as well as its generalized version (GEA). The two approaches differ in that the latter takes into account in the NN scattering amplitude the removal energy of the struck nucleon, or, equivalently, the excitation energy of the system $(A - 1)$.

The main results of our realistic and parameter free calculations can be summarized as follows:

- i) The agreement between the results of our calculations and the experimental data for both ${}^3\text{He}$ and ${}^4\text{He}$, is a very satisfactory one, particularly in view of the lack of any adjustable parameter in our approach.
- ii) In the kinematical range we have considered, only minor numerical differences were found between the conventional Glauber-eikonal approach and its generalized extension.
- iii) The effects of the FSI are such that they systematically bring theoretical calculations in better agreement with the experimental data.
- iv) Both for ${}^3\text{He}$ and ${}^4\text{He}$ the p_m dependence of the cross section exhibits peculiar slopes which can be interpreted in terms of multiple scattering effects; we have

firstly shown that in the ${}^4\text{He}$ case, the triple scattering starts to significantly contribute at $p_m \geq 800$ MeV/c.

- v) Finally, we investigated the Finite Formation Time (FFT) effects, which weakens the FSI at high Q^2 ; we found that available data on the ${}^4\text{He}(e, e'p)^3\text{H}$ process are only slightly affected by FFT effects, but, at the same time, similar data at higher Q^2 region such as $2 \leq Q^2 \leq 10$ (GeV/c) 2 around the dip region ($p_m \simeq 430$ MeV/c) would provide a significant check of theoretical models of FFT effects.

Final results of our calculations, including also a quantitative investigation of the limits of the validity of the factorized cross section, will be presented elsewhere [19].

Acknowledgments

L.P.K. and H.M. are indebted to the University of Perugia and INFN, Sezione di Perugia, for support and hospitality. H.M. also thanks the Grant of Sapporo Gakuin University for its financial support.

References

1. R. J. Glauber in *Lectures in Theoretical Physics* Vol. I p. 315 edited by W. E. Brittin and L. G. Dunham. (Wiley Interscience, New York, 1959).
2. V.N.Gribov, *Sov. Phys. JETP* **30**, 709 (1970).
3. L.L. Frankfurt, M.M. Sargsian and M.I. Strikman, *Phys. Rev. C* **56**, 1124 (1997).
4. M.M. Sargsian, T.V. Abrahamyan, M.I. Strikman and L.L. Frankfurt, *Phys. Rev. C* **71**, 044614 (2005).
5. C. Ciofi degli Atti and L.P. Kaptari, *Phys. Rev. C* **71**, 024005 (2005).
6. C. Ciofi degli Atti and L.P. Kaptari, *Phys. Rev. Lett.* **95**, 052502 (2005).
7. A. Kievsky, S. Rosati and M. Viviani, *Nucl. Phys. A* **551**, 241 (1993); A. Kievsky, *Private communication*.
8. R.B. Wiringa, V.G. Stokes and R. Schiavilla, *Phys. Rev. C* **51**, 38 (1995).
9. F. Benmokhtar *et al.*, *Phys. Rev. Lett.* **94**, 082325 (2005).
10. R. Schiavilla *et al.*, *Phys. Rev. C* **72**, 064003 (2005).
11. B. Reitz *et al.*, *Eur. Phys. J. A S* **19**, 165 (2004).
12. <http://pdg.lbl.gov> and <http://lux2.phys.va.gwu.edu>.
13. M.A. Braun, C. Ciofi degli Atti and D. Treleani, *Phys. Rev. C* **62**, 034606 (2000).
14. H. Morita, M. Braun, C. Ciofi degli Atti and D. Treleani, *Nucl. Phys. A* **699**, 328c (2002).
15. T. De Forest, Jr., *Nucl. Phys. A* **392**, 232 (1983).
16. M. Sakai, I. Shimodaya, Y. Akaishi, J. Hiura and H. Tanaka, *Prog. Theor. Phys. Suppl.* **56**, 32 (1974).
17. H. Morita, Y. Akaishi, O. Endo and H. Tanaka, *Prog. Theor. Phys.* **78**, 1117 (1987); H. Morita, Y. Akaishi and H. Tanaka, *Prog. Theor. Phys.* **79**, 1279 (1988).
18. I.E. Largaris and V.R. Pandharipande, *Nucl. Phys. A* **359**, 331 (1981).
19. C. Ciofi degli Atti, L. P. Kaptari and H. Morita, to appear.